Japan Geoscience Union Meeting 2015
(May 24th - 28th at Makuhari, Chiba, Japan)

SIT03-01 Room:106 Time:May 25 14:15-14:30

Synthesize of boron-doped diamond cylinder as a heater in Multi-anvil apparatus

XIE, Longjian[1*] ; YONEDA, Akira[1] ; ITO, Eiji[1]

[1]ISEI, Okayama University

Diamond is the hardest known material in the world. It is the first time to report synthesize of semi-conductor boron-doped diamond cylinder in the Kawai-type multi-anvil apparatus at 15 GPa and 2100^{o}C. The dimension of the cylinder is 2.6 mm outer diameter, 1.5 mm inner diameter and 3.35 mm length. SEM image shows that the grain size of diamond is about 1 micrometer.

Those cylinders have been used for extremely high temperature generation (~3000^{o}C) in a large sample volume (~0.1mm^{3}) in the Kawai apparatus; the sample volume is ~1000 times larger than that in diamond anvil cell. High X ray transparency of boron-doped diamond is optimum as well for in-situ synchrotron X ray analysis. Although there have been several reports on boron-doped graphite heater, the present study is the first report on pure boron-doped diamond heater in Kawai-type apparatus. The reversibility of the heater was confirmed well through three times of repeated cycle of heating and cooling. The boron-doped diamond heater with 3 wt.% boron shows metallic behavior, i.e. increasing resistance with increasing temperature. This electrical characteristic is beneficial for stably generating temperature as high as 2700^{o}C; the heating for higher temperature was failed because of failure of electrode. Therefore, succeeding optimization is required for higher temperature generation with this new heating element. Boron-doped diamond heater is more advantageous than B-doped graphite heater, because it is free from complicated power-temperature relationship and pressure drop associated with graphite to diamond conversion.

Keywords: diamond synthesize, B-doped diamond heater, ultrahigh temperature, Multi-anvil apparatus

Japan Geoscience Union Meeting 2015
(May 24th - 28th at Makuhari, Chiba, Japan)

SIT03-02 Room:106 Time:May 25 14:30-14:45

Electrical conductivity of San Carlos clinopyroxene as a function of water content

ZHAO, Chengcheng[1*] ; YOSHINO, Takashi[1]

[1]Institute for Study of the Earth Interior, Okayama University, Misasa, Tottori, 682-0193, Japan.

The high conductive region (50-100 km) obtained from magnetotelluric data at Southern East Pacific Rise has been interpreted by the high electrical conductivity of hydrous olivine. Though the fact that water could enhance the electrical conductivity orders of magnitude, the conductivity enhanced by hydrous olivine and orthopyroxene seems to be insufficient to account for this anomaly convincingly. Clinopyroxene, one of the main constituent minerals in the upper mantle, could be a possible candidate to raise the conductivity in this region because water tends to partition into this phase rather than olivine and orthopyroxene. In this study, we measured the electrical conductivity of clinopyroxene as a function of temperature and water content under the *P-T* condition corresponding to the conductivity anomaly region in the upper mantle.

Clinopyroxene aggregates with water contents ranging from ~0 to 2000 wt. ppm were synthesized from Scan Carlos clinopyroxene powder at 1270-1370 K and 1.5 GPa in a piston cylinder apparatus. The double capsule technique was used to realize the Ni-NiO buffer. The electrical conductivity measurements were performed at the same pressure and temperatures from 600 to 1200 K at the same oxygen fugacity, using a DIA-type apparatus. The water content of the sample both before and after electrical conductivity were determined by FTIR using Paterson calibration.

The electrical conductivity increases with increasing water content. Two conductive mechanisms were identified, i.e. proton conduction and hopping conduction. For hopping conduction, the activation energy is ~1.44 eV. For proton conduction, the activation energy differs by water content. At low water content, the activation energy is 1.28-1.36 eV; while at high water content, the activation energy is ~0.92 eV. All these data were fitted using the formula $\sigma=\sigma_{h0}\exp(-H_h/kT)+\sigma_{p0}C_w{}^r\exp(-H_p/kT)$. Compared with the electrical conductivity of olivine (Yoshino et al., 2006) and orthopyroxene (Zhang et al., 2012) under the same oxygen fugacity, electrical conductivity of hydrous clinopyroxene is comparable to those of the other major constitute minerals. To estimate electrical conductivity beneath the oceanic lithosphere as a function of water content, the Hashin-Shtrikman lower and upper bounds were used, and water-partitioning coefficients among olivine, orthopyroxene and clinopyroxene were also assumed. The model showed no obvious advantage to explain the high conductive anomaly. Thus, the conductivity anomaly predicted near the mid-ocean ridge cannot be originated from hydrated mantle. The conductivity anomaly region beneath the oceanic lithosphere should be explained by a presence of other conductive agents such as partial melt.

Yoshino et al. (2006), *Nature* **443**, 973-976.
Zhang et al. (2012), *EPSL* **357-358**, 11-20.

Keywords: clinopyroxene, electrical conductivity, water content, conductivity anomaly region, oceanic lithosphere

Japan Geoscience Union Meeting 2015
(May 24th - 28th at Makuhari, Chiba, Japan)

SIT03-03 Room:106 Time:May 25 14:45-15:00

Defect chemistry and diffusion in hydrous forsterite

FEI, Hongzhan[1*] ; KATSURA, Tomoo[2]

[1]Institute for Study of the Earth Interior, Okayama University, Misasa, Tottori, 682-0193, Japan, [2]Bayerisches Geoinstitut, University of Bayreuth, 95447, Bayreuth, Germany

The mass transport of olivine, which reflects the flow in the Earth's upper mantle, is controlled by the diffusion of structural elements. On the other hand, the diffusivity of an ion in the crystal is dominated by the motion of point defects of the corresponding sites. It is thus necessary to know the diffusivities of elements in olivine in the view of defect chemistry so as to investigate the behaviors in the upper mantle conditions.

Fei et al. (2013, 2014) systematically measured silicon and oxygen self-diffusion coefficients (D_{Si} and D_O, respectively) in iron-free forsterite as functions of water contents, showing that $D_{Si} \propto C_{H2O}{}^{0.32(7)}$, $D_O \propto C_{H2O}{}^{0.05(6)}$. These water-content exponents are much smaller than that expected on the basis of the assumption that self-diffusion coefficient of a chemical species is simply proportional to its defect density. Therefore, a new defect chemistry model is required to explain the above relationships.

Silicon diffusion:

The D_{Si} should be proportional to the density of silicon defects, namely, $D_{Si} \propto [V_{Si}'''']$. On the other hand, Si^{4+} is tightly surrounded by four-coordinated O^{2-}, and therefore, migration of Si^{4+} should be enhanced if a surrounding O^{2-} is missing. We can expect that a certain proportion of V_{Si}'''' is associated with $V_O^{\bullet\bullet}$ due to their excess charges with the opposite signs. As a result, Si migration is probably dominated by $V_O^{\bullet\bullet}$ -associated V_{Si}''''. D_{Si} is thus also proportional to $[V_O^{\bullet\bullet}]$ and we have,

$D_{Si} \propto [V_{Si}''''] \times [V_O^{\bullet\bullet}]$.

Under the charge neutrality condition of $[(OH)_O^{\bullet}] = 2[V_{Mg}'']$ in hydrous forsterite, we have $[V_{Si}''''] \propto (f_{H2O})^{2/3}$ and $[V_O^{\bullet\bullet}] \propto (f_{H2O})^{-1/3}$. Therefore,

$D_{Si} \propto [V_{Si}''''] \times [V_O^{\bullet\bullet}] \propto (f_{H2O})^{1/3}$,

which agrees well with the experimental results: $D_{Si} \propto (C_{H2O})^{0.32(7)}$ (Fei et al., 2013).

Oxygen diffusion:

In hydrous olivine/forsterite, hydrogen exists as hydroxyl, $(OH)^-$. Oxygen ions could diffuse either by hopping of O^{2-} without H^+ or by hopping of O in $(OH)^-$. Because H+-associated O has a lower Coulomb force due to the excess charge by H^+, the hopping probability of $(OH)^-$ should be higher than that of O^{2-}. Thus, the O diffusion should be dominated by O^{2-} of $(OH)^-$. As a result, we have,

$D_O \propto [V_O] \times ([O^{2-}]^{hopping} + [(OH)^-]^{hopping}) \approx [V_O^{\bullet\bullet}] \times [(OH)^-]^{hopping}$.

There are mainly three types of (OH)- in hydrous olivine/forsterite: (a) $(OH)_O^{\bullet}$ associated with V_{Mg}''; (b) $(OH)_O^{\bullet}$ associated with V_{Si}''''; (c) $(OH)_O^{\bullet}$ un-associated with any cation vacancies. The un-associated $(OH)_O^{\bullet}$ should have much higher mobility than V_{Si}'''' or V_{Mg}'' associated ones due to the Coulomb force and therefore the O diffusion is probably dominated by un-associated $(OH)_O^{\bullet}$. Thus,

$D_O \propto [V_O^{\bullet\bullet}] \times [(OH)^-]^{hopping} \approx [V_O^{\bullet\bullet}] \times [(OH)_O^{\bullet}]^{un-associated}$.

Under the charge neutrality condition of $[(OH)_O^{\bullet}] = 2[V_{Mg}'']$, we have $[V_O^{\bullet\bullet}] \propto (f_{H2O})^{-1/3}$ and $[(OH)_O^{\bullet}]^{un-associated} \propto (f_{H2O})^{1/3}$. Therefore,

$D_O \propto [V_O^{\bullet\bullet}] \times [(OH)_O^{\bullet}]^{un-associated} \propto (f_{H2O})^0$.

This model suggests that D_O is independent from C_{H2O}, which agrees well with the experimental results, $D_O \propto C_{H2O}{}^{0.05(6)}$ (Fei et al., 2014).

Fei et al. (2013), *Nature* **498**, 213-215.
Fei et al. (2014), *JGR* **119**, 7598-7606.

Keywords: defect chemistry, self-diffusion coefficient, silicon, oxygen, water content, forsterite

Japan Geoscience Union Meeting 2015
(May 24th - 28th at Makuhari, Chiba, Japan)

SIT03-04 Room:106 Time:May 25 15:00-15:15

D/H exchange in wadsleyite and ringwoodite: Implications for electrical conductivity

SUN, Wei[1*] ; YOSHINO, Takashi[1] ; SAKAMOTO, Naoya[2] ; YURIMOTO, Hisayoshi[2]

[1]ISEI, Okayama University, Misasa, Tottori 682-0193, Japan, [2]Division of Earth and Planetary Sciences, Hokkaido University, Sapporo, Hokkaido 060-0810, Japan

Wadsleyite and ringwoodite, which are main constituent minerals of the mantle transition zone, can incorporate large amount of hydrogen in their structure (up to a few wt % H2O). A knowledge of hydrogen self-diffusion in these minerals and its relationship with their electrical conductivity is critical to estimate the real amount of water present in the transition zone. Although only the hydrogen incorporation experiments in wadsleyite was performed using polycrystalline samples, the obtained diffusion coefficients cannot rule out the influence of grain boundary diffusion (Hae et al. 2006). Therefore, we have to investigate hydrogen lattice self-diffusion of wadsleyite and ringwoodite using single crystal at high pressure.

To estimate proton conduction from hydrogen self-diffusion, large single crystals (>1mm) of hydrogen (H) and deuterium (D)-doped wadsleyite and ringwoodite were synthesized respectively at high pressure and high temperature in Kawai-type multi-anvil apparatus.

We applied H/D exchange method to determine hydrogen self-diffusion coefficients because this method (Du Frane et al. 2012) has advantage to distinguish between incorporation and self-diffusion, and provides more accurate hydrogen diffusion coefficients contributing to proton conduction than traditional incorporation method (Kohlstedt and Mackwell, 1998, Demouchy and Mackwell, 2003, Hae et al. 2006).

After determination of crystallographic orientation, a pair of H and D-doped wadsleyite or ringwoodite crystals aligned to the same axis was placed together in gold capsule. The polished surfaces were tightly contacted each other. The inter-diffusion experiments were conducted at different temperatures (900-1300K) and the same pressure as synthesis condition. H/D inter-diffusion profiles were obtained by SIMS in Hokkaido University.

Hydrogen volume diffusion coefficients in wadsleyite determined from each single crystal pair are ˜1 order of magnitude lower than those obtained from polycrystal wadsleyite (Hae et al. 2006). The hydrogen self-diffusion coefficients in ringwoodite are characterized by lower enthalpy and hydrogen mobility than wadsleyite at the temperature of transition zone.

Electrical conductivities of wadslyite and ringwoodite estimated from the present diffusion coefficients based on the Nernst-Einstein relation. Our model suggests that hydrogen makes significant contributions to wadsleyite but insignificant contributions to ringwoodite due to large contribution of hopping conduction at the transition zone condition. Our proton conductivity values of wadsleyite are similar with those of Yoshino et al. [2012] at the transition zone condition but values of ringwoodite are lower especially at high water content. This model suggests that global average concentration of hydrogen in the transition zone of is ˜1000 wt ppm H2O.

Keywords: hydrogen, diffusion, wadsleyite, conductivity, ringwoodite

Japan Geoscience Union Meeting 2015
(May 24th - 28th at Makuhari, Chiba, Japan)

SIT03-05 Room:106 Time:May 25 15:15-15:30

Thickness of the mantle transition zone beneath the Society hotspot

SUETSUGU, Daisuke[1*] ; SUGIOKA, Hiroko[1] ; ISSE, Takehi[2] ; ITO, Aki[1] ; SHIOBARA, Hajime[2]

[1]Japan Agency for Marine-Earth Science and Technology, [2]Earthquake Research Institute, the University of Tokyo

We have conducted a seafloor geophysical observation from 2009 to 2010 near
the Society hotspot. The observation network was composed of nine sets of
broadband seismographs and electro-magnetometers, and two differential pressure gauges. In this presentation we show the mantle transition zone (MTZ) structure obtained with a receiver function method using the broadband seismograms. We employed a common-conversion point (CCP) stacking technique to map the MTZ thickness. A preliminary result indicates an area of a thin MTZ 200 km to the south of the Society hotspot (thinner than global average by 20-30 km). The lateral dimension of the thin MTZ area is about 200 km. There is another area of the thin MTZ 300 km EES to the hotspot. The thin MTZ areas are roughly correlated with slow P-velocities in the MTZ in the P-wave tomograms (Obayashi et al., 2014). They may represent hot mantle plumes ascending from the lower mantle.

Keywords: hotspot, ocean bottom seismograph, receiver function, French Polynesia

Japan Geoscience Union Meeting 2015
(May 24th - 28th at Makuhari, Chiba, Japan)

SIT03-06 Room:106 Time:May 25 15:30-15:45

Experimental Study on the Hawaiian Plume with Recycled Eclogite: Part-1: Constraints on potential temperature

TAKAHASHI, Eiichi[1*] ; GAO, Shan[1]

[1]Magma Factory, Earth and Planetary Sciences, Tokyo Institute of Technology

Potential mantle temperatures (PMT) of plumes are thought to be significantly higher than shallow asthenosphere (200˜300C). Excess PMT of the plume is very important in calculating the plume flux among the heat budget of the Earth dynamics (e.g., Sleep, 1990). In order to produce large amount of tholeiite magma in the shield building stage at the base of old Pacific plate, potential temperature of the Hawaiian plume is considered to be at least 300C higher than asthenosphere judging from the peridotite dry solidus at 3 GPa, base of the oceanic plate (e.g., Watson & McKenzie, 1991).

If large amount of recycled eclogite component is involved in the genesis of LIP magmas (e.g., Hawaii hot spot: Hauri, 1996; Takahashi & Nakajima, 2002, Sobolev et al., 2007, Columbia River flood basalt: Takahashi et al., 1998), PMT of the plumes which have been estimated based on peridotite dry solidus alone should be largely in error. For example, Takahashi et al.(1998) concluded that temperature of the initial emplacement stage of the Yellowstone plume may be only 100C higher than normal asthenosphere, based on melting study of the Columbia River basalts. In order to evaluate the role of recycled eclogite in magma genesis of Hawaiian plume, we carried out hig-P and high-T melting experiments. Chemistry of the recycled eclogite will be discussed in Part 2.

High-pressure melting experiments were carried out under dry and hydrous conditions with layered eclogite/peridotite starting materials. Spinel lherzolite KLB-1 (Takahashi 1986) was employed as peridotite component in this study. Two basalt components were tested as recycled crust component: 1) Columbia River basalt (CRB72-180, Takahashi et al., 1998) which is relatively enriched in K, Ti and LREE (K2O?1wt%, TiO2=3.15wt%), N-type MORB (NAM-7, Yasuda et al., 1994) (for REE patterns, see Fig.1 of Gao et al. this conference, Part 2 of this work). The 2.85GPa experiments (corresponding to about 80km depth which is the top most horizon of the Hawaiian plume head) were carried out with Boyd-England type piston-cylinder apparatus at (1460˜1540C for dry experiments; 1400˜1500C for hydrous experiments), The 5GPa experiments (corresponding to about 150km depth on the plume axis) were conducted by Kawai-type multi-anvil apparatus (1550˜1650C for dry experiments; 1350˜1550C for hydrous experiments).

Melts formed by reactive melting of dry eclogite and peridotite changes dramatically in the temperature range across the solidus of peridotite KLB-1 from basalt (below dry solidus) to picrite (20-40C above dry solidus). Basaltic melts are not saturated with olivine both at 2.85 and 5 GPa and therefore they are separated by peridotite matrix by Opx film. Chemical reaction between the basalt melt and the peridotite matrix proceeds only slowly by solid-diffusion across the Opx film. In hydrous experiments, solidus of peridotite decreases significantly and therefore the reaction between hydrous melt and the partially molten peridotite matrix proceeds at temperatures below peridotite dry solidus.

Based on present experiments, we propose that potential temperature of the Hawaii plume may be only 100-150C above that of normal asthenosphere. Tholeiite magma in the shield building stage may be formed slightly under hydrous condition near the dry solid of peridotite (1450-1500C at about 3 GPa). Chemical distinction between Hawaiian shields (e.g., Mauna Loa and Kilauea) might correspond with difference in mixing ratio or degree of the chemical reaction between the recycled eclogite blocks and the ambient peridotite.

Potential mantle temperature in other mantle plume (OIB, flood basalt, etc) will be discussed in the light of present experiments. Our model predicts lower plume temperatures than most previous estimates. Plume flux may be related to the amount of entrained eclogite than potential temperature.

Keywords: Hawaiian plume, recycled eclogite, magma genesis, potential temperature

Japan Geoscience Union Meeting 2015
(May 24th - 28th at Makuhari, Chiba, Japan)

SIT03-07 Room:106 Time:May 25 15:45-16:00

Experimental Study on the Hawaiian Plume with Recycled Eclogite: Part 2, Constraints on Chemistry of Recycled Component

GAO, Shan[1*] ; TAKAHASHI, Eiichi[1] ; KIMURA, Jun-ichi[2] ; SUZUKI, Toshihiro[1]

[1]Earth & Planetary Sciences, Tokyo Institute of Technology, [2]Department of Solid Earth Geochemistry,Japan Agency for Marine-Earth Science and Technology

Introduction: It is believed that recycled oceanic crust is involved in the magma genesis of the Hawaiian mantle plume (e.g., Hauri et al., 1996; Takahashi & Nakajima., 2002; Sobolev et al., 2007). Takahashi & Nakajima (2002) proposed that magma produced near the axis of the plume head may be mixtures of two types of melts 1) basaltic andesite melt formed by melting of eclogite and 2) picritic melts formed by the reactive melting of eclogite and peridotite. However, geochemical feature of recycled oceanic crust component is still under disputed. A sequence of high-T high-P experiments were conducted to figure out constrains of such recycled component. Experimental details are shown in Part 1 of this presentation.

Phase and major elements features:

1) Anhydrous conditions: (CRB: 1460˜1540C, 3h for 2.85GPa; N-MORB or CRB: 1550˜1650C for 5GPa):

When peridotite remained subsolidus, molten basalt was separated from peridotite by thin Opx band formed by the chemical reaction between Si-rich partial melt of eclogite and olivine in the peridotite matrix, therefore the chemical reaction between basalt and peridotite layers proceeded only by solid diffusion. As peridotite reached its solidus between 1520C˜1540C, fully molten basalt melt and melt pockets from peridotite layer linked, judging from sharp changes in MgO and FeO/MgO ratio. Extensive chemical mass transport took place by chemical diffusion and liquid percolation. However, Si-content remained nearly constant even at temperatures above solidus.

2) Hydrous conditions: 1400C˜1500C, 2.85GPa 3h

In wet experiments (with 1wt% H_2O in peridotite layer originally), extraction of water took place from peridotite layer into basaltic melt (water was detected by FT-IR), giving little influence to the melting process of peridotite. On the other hand, in wet experiments (with 5wt% H_2O in peridotite layer), basalt started melting even at 1400?C. At 1480C and 1500C, melting process of both layers enhanced the chemical exchange of both sides. H_2O promotes melting of only basalt layer under low water concentration, while it enhances melting and chemical interaction between both layers leading to formation of Si-poor melts in basalt.

In the case 5GPa, 1wt% H_2O, coexisted hydrous vapor and hydrous silicate melt generated under temperature 1350˜1450C (about 200C below peridotite dry solidus). Ti, K, P are enriched in the hydrous vapor.

REE features.

Rare earth element patterns: Columbia River basalt is enriched in LREE than N-MORB, run products of this study turned out to have a similar pattern (Fig.1, normalized patttern by CI chondrite)) with their starting material (basalt). Since REE elements prefer to stay in the melt, increasing degree of partial melting will lower the whole REE elements abundance in the melt. REE abundance of lava from Kilauea and Mauna Loa is also plotted in this diagram, showing sharp decline of HREE components in these shield stage lava. Garnet (the key component of eclogite) is the only known mineral that prefers heavy REE. Although garnet together with Cpx are the residual phase at 2.85 and 5 GPa experiments, REE patterns of Kilauea and Mauna Loa are far more depleted in HREE than melts produced by our experiments. .

Discussion: In an upwelling mantle plume with recycled oceanic basalt components, both tholeiitic magma and alkali component could be obtained from hybrid melting of basalt and peridotite. H_2O promotes the melting process and generate more mafic melts. Very depleted HEE pattern of Hawaiian tholeiite might be explained by percolation of partial melt in vertically elongated eclogite blobs in the center of the plume (chromatographic effect). Enriched signature in K , Ti, and LREE in the Hawaiian tholeiite might indicate that source of recycled component in the Hawaiian plume is not NMORB but is more enriched in these incompatible elements (see Fig.1).

Keywords: Hawaii plume, magma genesis, recyled eclogite, chemistry, REE

SIT03-07 Room:106 Time:May 25 15:45-16:00

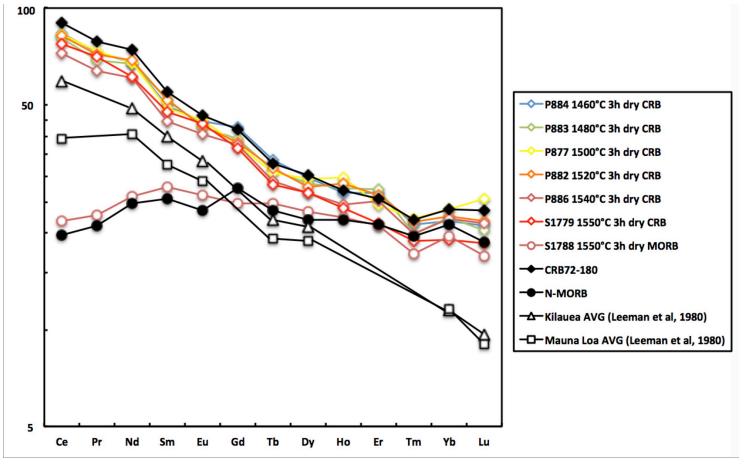

Japan Geoscience Union Meeting 2015
(May 24th - 28th at Makuhari, Chiba, Japan)

SIT03-08 Room:106 Time:May 25 16:15-16:30

High-pressure and high-temperature polymorphism in the CaCO3 at pressures to 30 GPa

LITASOV, Konstantin[1*] ; SHATSKIY, Anton[1] ; SHARYGIN, Igor[1] ; CHANYSHEV, Artem[2] ; GAVRYUSHKIN, Pavel[2] ; BEKHTENOVA, Altyna[2]

[1]VS Sobolev Institute of Geology and Mineralogy, Novosibirsk, Russia, [2]Novosibirsk State University, Novosibirsk, Russia

We determined phase transitions in $CaCO_3$ at pressures up to 30 GPa and high-temperatures using *in situ* X-ray diffraction and synchrotron radiation. In additional to geological importance this investigation has crystal-chemical and fundamental aspect as in this region enigmatic phase transitions from aragonite to disordered calcite or other phases takes place. The degree of orientational disorder in calcite drastically grow in the narrow temperature range of 1200-1230 K (at 1 bar) producing fully disordered phase (by orientation of CO_3 triangles) (Ishizawa et al., 2013). Despite of such apparent significance, there is just a few works where this phase transition was investigated by X-ray diffraction at high pressures (Suito et al., 2001). The results are not unequivocal, because disordered calcite was determined by only common similarity of diffraction patterns, whereas unit cell parameters were not determined. By the same reason the compressibility of disordered calcite is also unknown. The lack of the experimental results is explained by grain growth and disordering phase transitions in $CaCO_3$ at temperatures close to the melting point and as a result difficulties in getting relatively high quality diffraction patterns with amount of peaks enough for unit cell parameters determination. In present experiments we observed transition of aragonite to presumably disordered calcite phase at 1 and 3 GPa and 1273-1473 K, however at 5 and 8 GPa and higher temperature we observed transition to new phase, which we tentatively named disordered aragonite. At 14 GPa we did not observe transition of aragonite in the experiment to 1900 K, however at 20 GPa and at 31 GPa transition from aragonite to new phase(s) was observed at 1773 and 1373 K, respectively. The structures of the new phases will be refined based on diffraction data and subsequent *ab initio* computations.

Keywords: high pressure, calcium carbonate, phase transition, aragonite, X-ray diffraction

Japan Geoscience Union Meeting 2015
(May 24th - 28th at Makuhari, Chiba, Japan)

SIT03-09 Room:106 Time:May 25 16:30-16:45

High-pressure decomposition of FeTiO3, MgTiO3 and ZnTiO3 perovskites

AKAOGI, Masaki[1*] ; ABE, Kohei[1] ; ISHII, Takayuki[1] ; KOJITANI, Hiroshi[1] ; YUSA, Hitoshi[2]

[1]Department of Chemistry, Gakushuin University, [2]National Institute of Materials Science

It is generally accepted that transition of $MgSiO_3$-rich perovskite (bridgmanite) to $CaIrO_3$-type postperosvkite is responsible for formation of D" layer in the lowermost mantle. Since discovery of the perovskite-postperovskite transition in $MgSiO_3$, numerous studies have been made to clarify high-pressure transitions of ABX_3 perovskites. $FeTiO_3$ and $MgTiO_3$ are endmembers of natural ilmenite, and $ZnTiO_3$ is an analogue for these compounds. Previous studies revealed that at 15-20 GPa range $FeTiO_3$ and $MgTiO_3$ ilmenites transform to perovskites, which are recovered as $LiNbO_3$-type phases at ambient conditions. In contrast to many perovskite-type oxides including $MgSiO_3$ perovskite, $FeTiO_3$ and $MgTiO_3$ perovskites do not transform to $CaIrO_3$-type postperovskite but decompose into two-phase assemblages. However, the transition behaviors of these perovskites are still in controversy, and little has been known on phase transition of $ZnTiO_3$.

We have examined high-pressure transitions in $ZnTiO_3$ and $MgTiO_3$ to about 25 GPa and those of $FeTiO_3$ to about 33 GPa using multianvil apparatus. Pressure was calibrated against press-load using pressure-fixed points at room temperature including GaP and Zr. The pressure was further corrected at high temperature using transition boundaries including dissociation of pyrope into Mg-rich perovskite + corundum. Quenched samples were examined by powder X-ray diffractometers and a scanning electron microscope with an energy-dispersive X-ray spectrometer. Some in-situ X-ray observations on $ZnTiO_3$ phases have also been made using a diamond anvil cell with synchrotron X-ray diffraction method.

The results by quench and in-situ experiments on $ZnTiO_3$ indicate that at 1200 ^oC $ZnTiO_3$ ilmenite transforms to perovskite at 10 GPa, which dissociates into rocksalt-type ZnO + baddeleyite-type TiO_2 at 22 GPa. On release of pressure, perovskite-type $ZnTiO_3$, rocksalt-type ZnO and baddeleyite-type TiO_2 are converted into $LiNbO_3$-type, wurtzite-type and αPbO_2-type phases, respectively. $MgTiO_3$ perovskite decomposes into MgO + baddeleyite-type TiO_2 at 20 GPa and 1400 ^oC. $FeTiO_3$ perovskite dissociates first into $CaTi_2O_4$-type Fe_2TiO_4 + TiO_2 phase at about 28 GPa. At about 30 GPa, this assemblage further changes into $Fe_3Ti_2O_7$ phase + TiO_2 phase below about 1100 ^oC, above which $CaTi_2O_4$-type Fe_2TiO_4 + $FeTi_2O_5$ phase were synthesized. These two assemblages have not yet been found in the previous studies. Combination of our results on $ZnTiO_3$, $MgTiO_3$ and $FeTiO_3$ with those of other titanate perovskites suggests that transition pressure of titanate perovskite increases with tolerance factor or ionic radius of divalent cation. It is also indicated that all the titanate perovskites studied dissociate into two-phase assemblages which are denser than hypothetical $CaIrO_3$-type postperovskites. This is consistent with the previously suggested tendency that ABX_3 perovskites with relatively ionic B-X bonds do not transform to postperovskites.

Keywords: perovskite, titanate, high pressure experiment, postperovskite

Japan Geoscience Union Meeting 2015
(May 24th - 28th at Makuhari, Chiba, Japan)

SIT03-10 Room:106 Time:May 25 16:45-17:00

Phase relations of MgSiO3-Al2O3 system in Earth's lower mantle

LIU, Zhaodong[1*] ; IRIFUNE, Tetsuo[1] ; NISHI, Masayuki[1] ; TANGE, Yoshinori[2] ; ARIMOTO, Takeshi[1] ; SHINMEI, Toru[1]

[1]Geodynamics Research Center (GRC), Ehime University, [2]Spring-8, Japan Synchrotron Radiation Institute

Abstract

Aluminum oxide (Al_2O_3) is present in about 4~5 mol% for the Earth's mantle compositions, e.g., pyrolite, piclogite and chondrite (Ringwood, 1966; Sun, 1982; Anderson, 1989; Irifune et al. 1986, 2007). In the Earth's uppermost parts of lower mantle conditions, the Al_2O_3 is accommodated mainly in bridgmanite (Irifune 1994), which is the most abundant mineral phase in this region (Ringwood 1975). The $MgSiO_3$-Al_2O_3 system is a basis system to understand lower mantle phase equilibria in a more complex composition. Phase relations of $MgSiO_3$-Al_2O_3 system have since been extensively studied using the multi-anvil apparatus with tungsten carbide anvils from upper mantle to the uppermost parts of lower mantle conditions (Irifune 1986, 1996; Kubo et al. 2000; Hirose et al. 2001; Akaogi et al. 2002), and also further constructed by theoretical calculation (Panero et al. 2006; Tsuchiya et al. 2008). The phase relation of $MgSiO_3$-Al_2O_3, especially toward the Al_2O_3-rich side, in the lower mantle conditions is still relatively limited. Recent technique development of sintered diamond anvils in multi-anvils apparatus allow us to achieve the high pressures and high temperatures conditions of Earth's middle lower mantle(Tange et al. 2008, 2009; Irifune et al. 2010; Ito et al. 2010; Nishi et al. 2013; Yamazaki et al. 2014). Here, we further extend the phase relations of $MgSiO_3$-Al_2O_3 system between 31 GPa and 45 GPa at 2000 K using multi-anvil apparatus with sintered diamond anvils. Aluminum oxide solubility in bridgmanite is increasing with increasing pressure and temperature. These results can further confirmed previous experimental studies on the same system and pyrolite composition (Irifune et al. 1994, 1996, 2010), and the entire inventory of Al_2O_3 in pyrolite can be accommodated in bridgmanite in Earth's lower mantle.

Keywords: Aluminum oxide, bridgmanite, lower mantle, sintered diamond technique, phase relation

Japan Geoscience Union Meeting 2015
(May 24th - 28th at Makuhari, Chiba, Japan)

SIT03-11 Room:106 Time:May 25 17:00-17:15

First principles study on the phase stability and elasticity of potassium-host hexagonal aluminous phases

KAWAI, Kenji[1*] ; TSUCHIYA, Taku[2]

[1]Department of Earth Science and Astronomy, Graduate School of Arts and Sciences, University of Tokyo, [2]Geodynamics Research Center, Ehime University

In order to understand the fate of the potassium-bearing phase subducted into the deep Earth's interior, we have studied the high-pressure stability and elasticity of KMg2Al5SiO12 hexagonal aluminous phase (K-Hex) by means of the density functional computation method. The K-Hex phase is found to be mechanically stable up to 150 GPa and also energetically more stable than the calcium-ferrite (K-CF) type structure up to 150 GPa. In addition, calculations indicate that when the spinel composition coexists with the K-hollandite (K-Hol) phase, the K-Hex phase becomes more stable than the K-Hol phase at pressures above ~27 GPa. This suggests that the hexagonal aluminous phase be a potential host of the incompatible large-ion elements such as potassium in the lower mantle, especially in the subducted basaltic Mg and Al rich composition. Finally, seismic velocities of the K-Hex phase are found slower than Mg-perovskite (pv) in the lower mantle pressures, while its density is larger than Mg-pv over 70 GPa

Keywords: High pressure, Pottasium, Lower mantle, Aluminous phase

Japan Geoscience Union Meeting 2015
(May 24th - 28th at Makuhari, Chiba, Japan)

SIT03-12 Room:106 Time:May 25 17:15-17:30

Effect of Al content on electrical conductivity of bridgmanite

YOSHINO, Takashi[1*] ; KAMADA, Seiji[2] ; OHTANI, Eiji[2] ; HIRAO, Naohisa[3]

[1]Institute for Study of the Earth's Interior, Okayama Univ., [2]Tohoku Univ., [3]JASRI

Electrical conductivity is one of useful methods to prove temperature, structure and composition of the Earth's deep interior. Interpretation of electrical conductivity in the Earth has been done by comparison between conductivities obtained from geophysical observations and conductivities measured in the laboratory. Because bridgmanite is believed to be a dominant constituent mineral in the lower mantle, knowledge of electric conduction for bridgmanite to constrain the conductivity profile of the lower mantle. Xu et al. (1998) reported that Al incorporation to bridgmanite enhance the electron hopping conduction. Although there is a large variation of Al content in bridgmanite under the lower mantle, electrical conductivity of aluminous bridgmanite have not been measured as a function of Al content.

In this study, Impedance spectroscopy measurements were performed at 26 or 28 GPa and up to 2000 K in a Kawai-type multi-anvil apparatus in order to investigate effect of aluminium content on electrical conductivity of bridgmanite. The starting materials were synthetic orthopyroxene ($Mg_{0.9}$, $Fe_{0.1}$)SiO_3 powders with various amounts of aluminium (Al_2O_3 = 3, 6 and 10 wt.%). Electrical conductivity of aluminous bridgmanite increases with increasing Al content. At temperatures below 1700 K, the activation enthalpies of these samples are around 0.4 eV, which is consistent with that reported by Shankland et al. (1993), who measured the conductivity of quenched perovskite. At higher temperatures ($>$1800 K) corresponding to temperature conditions of the uppermost lower mantle, the conductivity of samples with relatively lower Al content abruptly increases with temperature and the resultant activation enthalpy is around 1 eV, which is consistent with that reported by Dobson (2003). At temperatures below about 1700 K, small polaron (electron hole hopping between ferrous and ferric iron sites) conduction with activation energy of 0.4 eV is considered as a dominant conduction mechanism of aluminous bridgemanite. At higher temperatures, a different conduction mechanism dominates with more than1 eV of activation enthalpy.

To estimate ferric iron content in bridgmanite, synchrotron Mossbauer spectroscopy was performed at SPring-8 BL10XU. The ferric iron contents of all samples are estimated to be more than 60 % against total iron content. Proportion of ferric iron in A site tends to increase with increasing Al contents. Thus, increase of ferric iron content due to Al incorporation into bridgmanite can induce enhancement of conductivity. At high temperatures above 1800 K, the dominant conduction mechanism can change extrinsic oxygen ionic conduction when Al_2O_3 content is low. Xu and McCammon (2002) reported evidence that in aluminous perovskite with Mg#90, ionic conduction characterized by high activation energy (1.5 eV) becomes significant above 1700 K dependent on Al content. This is most likely due to the presence of oxygen vacancies, which charge-balance Al and ferric iron substituting onto the B site (Brodholt 2000; Lauterbach et al. 2000). The present results suggest that the electrical conductivity of a region at the top of the earth's lower mantle could be sensitive to amount of Al content in bridgmanite. On the other hand, when Al content in bridgmanite is low, the lower mantle conductivity will be more sensitive to temperature due to the extrinsic oxygen ionic conduction.

References

Brodholt, J.P., Nature 407, 620?622, 2000.
Dobson, D., 2003. Phys. Earth Planet. Inter. 139, 55-64, 2003.
Lauterbach, S., C. A. McCammon, P. van Aken, F. Langenhorst, F. Seifert, Contrib. Mineral. Petrol., 138, 17? 26, 2000.
Shankland, T.J., Peyronneau, J., Poirier, J.-P., Nature 366, 453?455, 1993.
Xu, Y., McCammon, C., Poe, B.T., Science282, 922?924, 1998.
Xu, Y., C. McCammon, J. Geophys. Res., 107, 2251, 2002.

Keywords: bridgmanite, lower mantle, electrical conductivity, Mosbauer spectrocopy, Al, electron hopping

Japan Geoscience Union Meeting 2015
(May 24th - 28th at Makuhari, Chiba, Japan)

SIT03-13 Room:106 Time:May 25 17:30-17:45

Toward the unified image of the spin transition of iron in the lower mantle

FUJINO, Kiyoshi[1*] ; IRIFUNE, Tetsuo[1]

[1]Geodynamics Research Center, Ehime University

The pressure-induced spin transition of iron in the lower mantle minerals deeply affects the structures and physical properties of the lower mantle minerals, and there by the dynamics of the lower mantle. So far, many experimental and theoretical studies have been carried out to clarify the spin transition of iron in the lower mantle minerals. However, there is still a controversy about the existence and the pressure dependence of the spin transition of iron in Mg-perovskite (Pv) and post-Mg-perovskite (PPv) at the lower mantle conditions. Pv and PPv in the lower mantle are considered to involve both Fe^{2+} and Fe^{3+}, and Al as minor elements. Until recently, the controversy had been mainly about the spin transition of Fe^{2+}. Now, the spin transition of Fe^{2+} in Pv and PPv seems to be settling down in the direction that Fe^{2+} in both Pv and PPv remains high spin (HS) at the dodecahedral site (A site) at the lower mantle conditions (Hsu et al., 2011; Yu et al., 2012).

On the other hand, with the spin transition of Fe^{3+} there are still large discrepancies among the reports, particularly related to the Al content involved in Pv and PPv. Some experimental results indicate that Fe^{3+} becomes low spin (LS) at the octahedral site (B site) in Al-bearing Pv (above ca. 70 GPa) and PPv (whole stability region) (Catalli et al., 2011; Fujino et al., 2012, 2013), while other experimental results indicate that Fe^{3+} coexisting with Fe^{2+} at the A site prefers to occupy the A site and remains HS even at high pressure (Mao et al., 2014; Dorfman et al., 2014). Meanwhile first-principles calculations indicate that Fe^{3+} remains HS at the A site in Al-bearing Pv and PPv (Hsu et al., 2012).

In the presentation, the possible explanations to resolve the above discrepancies among the previous reports to obtain the unified image of the spin transition of iron in the lower mantle minerals are proposed.

Keywords: spin transition of iron, ferric iron, Mg-perovskite, post-Mg-perovskite, Al content, cation exchange reaction

Japan Geoscience Union Meeting 2015
(May 24th - 28th at Makuhari, Chiba, Japan)

SIT03-14 Room:106 Time:May 25 17:45-18:00

Deep structure and seismic anisotropy of the Western-Pacific subduction zones

ZHAO, Dapeng[1*] ; WEI, Wei[1]

[1]Tohoku University, Department of Geophysics

We determined high-resolution P and S wave tomography and 3-D P-wave azimuthal anisotropy of the Western-Pacific subduction zones by inverting a large number of P and S wave arrival-time data of local and regional earthquakes. Our results show some differences between P and S wave images for the stagnant Pacific slab in the mantle transition zone (MTZ) beneath Northeast Asia. The stagnant slab looks thicker in the P wave image than that in the S wave image, which may reflects the effects of both hydration and lower temperature in the MTZ, though differences in the resolution of P and S wave tomography may also have some effects. The Changbai and other intraplate volcanoes in NE Asia are caused by hot and wet upwelling in the big mantle wedge above the stagnant Pacific slab in the MTZ. Our P-wave anisotropy tomography shows that the fast velocity direction (FVD) in the subducting Philippine Sea plate beneath the Ryukyu arc is NE-SW (trench parallel), which is consistent with the spreading direction of the West Philippine Basin during its initial opening stage, suggesting that it may reflect the fossil anisotropy. A striking variation of the FVD with depth is revealed in the subducting Pacific slab beneath the Northeast Japan arc, which may be caused by slab dehydration that changed elastic properties of the slab with depth. The FVD in the mantle wedge beneath the Northeast Japan and Ryukyu arcs is trench normal, which reflects subduction-induced convection. Beneath the Kuril and Izu-Bonin arcs where oblique subduction occurs, the FVD in the mantle wedge is nearly normal to the moving direction of the downgoing Pacific plate, suggesting that the oblique subduction together with the complex slab morphology have disturbed the mantle flow.

Keywords: Subduction zones, Seismic tomography, Anisotropy, Slab, Earthquakes

Japan Geoscience Union Meeting 2015
(May 24th - 28th at Makuhari, Chiba, Japan)

SIT03-15 Room:106 Time:May 26 09:00-09:15

Archean lithosphere in time and space: geophysical evidence on lateral and vertical heterogeneity in Siberia

ARTEMIEVA, Irina[1*] ; HERCEG, Matija[1] ; CHEREPANOVA, Yulia[1] ; THYBO, Hans[1]

[1]IGN, University of Copenhagen

We present geophysical models for Precambrian cratons, including the structure of the crust and the lithospheric mantle, and the thermal structure of the Precambrian lithosphere based on surface heat flow data. A particular focus is on thermo-compositional heterogeneity of the lithospheric mantle. It is modelled as a non-thermal part of upper mantle seismic velocity heterogeneity based on a joint analysis of thermal and seismic tomography data, and as lithosphere density heterogeneity as constrained by free-board and satellite gravity data. The results are compared with xenolith data from the Siberian kimberlite provinces.

An analysis of surface heat flow indicates that many Precambrian cratons (particularly Siberia) are characterized by extremely low surface heat flow (<25-30 mW/m2), which is in apparent contradiction with a worldwide compilation of cratonic xenolith P-T arrays. In regions with very low heat flow, the depth extent of the lithospheric keels locally may reach the depth of 300-350 km.

An analysis of temperature-corrected seismic velocity structure indicates strong vertical and lateral heterogeneity of the cratonic lithospheric mantle. The lateral extent of depleted lithospheric keels diminishes with depth and, below a 150-200 km depth, is significantly smaller than geological boundaries of the cratons. In the Siberian craton, Proterozoic sutures and intracratonic basins are manifested by an increase in mantle density as compared to light and strongly depleted lithospheric mantle of the Archean nuclei.

We demonstrate that density structure of the cratonic lithosphere is well correlated with crustal structure and surface tectonics. The analysis of lithosphere seismic velocity and density structure allows for speculations on processes which formed and modified the Archean lithosphere.

Keywords: craton, lithospheric mantle, density, lithosphere thickness, depletion, metasomatism

Japan Geoscience Union Meeting 2015
(May 24th - 28th at Makuhari, Chiba, Japan)

SIT03-16 Room:106 Time:May 26 09:15-09:30

Variable inertia method: A novel numerical method for mantle convection simulation

TAKEYAMA, Kosuke[1*] ; SAITOH, Takayuki[2] ; MAKINO, Junichiro[3]

[1]Tokyo Institute of Technology, [2]Earth-Life Science Institite, [3]RIKEN AICS

It is important to understand mantle convection in the earth and the 3D numerical simulation has been a very useful tool. In almost all previous simulations of the mantle convection, the anelastic approximation and the (extended) Boussinesq approximation has been used. An implicit method should be used to solve the equation of motion applied above approximations to allow the use of long timesteps not limited by the CFL condition. However, the resulting matrix is ill-conditioned, in particular since the viscosity depends strongly on the temperature. Thus, 3D simulation of the mantle convection is not well-suited to modern large-scale parallel machines. We have developed an explicit method which can be used to solve mantle convection problem.

Recently, Rempel (2005) proposed the reduced speed of sound technique (RSST) to solve the thermal convection of our Sun. Previously, an incompressible approximation was used to solve the convection of the Sun, as a result, an implicit method was used. The basic idea of RSST is, as its name suggest, modify the continuity equation to reduce the sound speed, thereby allowing the long timestep not limited by the physical CFL condition. Hotta et al. (2012) applied RSST to the thermal convection of our Sun. They confirmed that the characteristic of the flow is not changed as far as the Mach number is smaller than ˜0.7, and successfully performed the high resolution simulation of our Sun (Hotta et al. 2014, 2015).

Since not only Mach number, but also the Reynolds number is very small in the mantle, we developed a new formulation which can change these two numbers independently. In order to reduce the sound speed, we multiplied the inertia term of the equation of motion by a large and viscosity-dependent coefficient. We also scale the thermal conductivity and the viscosity in a consistent way so that the characteristic of the flow is unchanged. Using these two modifications, we can change the Mach number and Reynolds number independently. Theoretically, we can expect that this modification would not change the flow as far as the Reynolds number and the Mach number are sufficiently smaller than unity. We call this method the variable inertia method (VIM).

We have performed an extensive set of numerical tests of the proposed method for thermal convection, and confirmed that the characteristics of the flow are not changed by VIM. In particular, it can handle the difference of viscosity of more than five orders of magnitude. Since we can use the long timestep with VIM, we can finish a simulation much faster than that without VIM without losing accuracy. Our new scheme is well suited for simulations on modern large-scale parallel machines since it is an explicit method and thus it opens a new door to very high resolution simulations of mantle convection.

Keywords: mantle convection, numerical simulation

Japan Geoscience Union Meeting 2015
(May 24th - 28th at Makuhari, Chiba, Japan)

SIT03-17 Room:106 Time:May 26 09:30-09:45

Linear analysis on the onset of thermal convection of highly compressible fluids with variable physical properties

KAMEYAMA, Masanori[1*]

[1]Geodynamics Research Center, Ehime University

A series of linear analysis was performed on the onset of thermal convection in a highly compressible fluid with variable physical properties, in order to study the fundamental nature of mantle convection of massive super-Earths in the presence of strong adiabatic compression. We consider the temporal evolution (growth or decay) of an infinitesimal perturbation superimposed to a highly compressible fluid which is in a hydrostatic (motionless) and conductive state in a basally-heated horizontal layer. As a model of spatial variations in physical properties, we employed an exponential dependence of thermodynamic properties (thermal expansivity and reference density), together with the spatial variations in transport properties (thermal conductivity and viscosity). The linearized equations for conservation of mass, momentum and internal (thermal) energy are numerically solved for the critical Rayleigh number as well as the vertical profiles of eigenfunctions for infinitesimal perturbations. The above calculations are repeatedly carried out by systematically varying (i) the dissipation number which measures the effect of adiabatic compression, (ii) the temperature at the top surface and (iii) the magnitude of spatial variations in physical properties of the modeled fluid.

By first analyzing the roles of thermodynamic properties, we found that the onset of thermal convection is strongly affected by the adiabatic compression, through the modulation of the static stability of thermal stratification in the fluid layer. For sufficiently strong adiabatic compression where a very thick “stratosphere” of stable stratification develops in the layer, for example, the critical Rayleigh number explosively increases with the dissipation number. The explosive changes in the critical Rayleigh number are associated with drastic decreases in the length scales of perturbations both in vertical and horizontal directions. In addition, when the effect of adiabatic compression is extremely strong so that the thermal stratification becomes stable in the entire layer, no perturbation is allowed to grow with time regardless of the Rayleigh number and/or the horizontal wavelength.

We also found that the critical states of thermal convection are greatly altered by introducing the depth-dependence in thermal conductivity: the increase in thermal conductivity counteracts the decrease in thermal expansivity with depth by raising the adiabatic temperature change and, hence, enhancing the stability of thermal stratification. In particular, for the cases where a “stratosphere” occurs at the mid-depth of the fluid layer owing to the moderate depth-dependence both in thermal expansivity and conductivity, we observed discontinuous changes in the structures of incipient flows with the dissipation number, depending on the concentration of flows either in the upper and lower “tropospheres”. Our findings suggest that a delicate interplay between the depth-dependent thermal expansivity and conductivity is of crucial importance in understanding the dynamic nature of the mantle convection of massive super-Earths.

Keywords: super-Earths, mantle convection, adiabatic compression, thermal expansivity, thermal conductivity

Japan Geoscience Union Meeting 2015
(May 24th - 28th at Makuhari, Chiba, Japan)

SIT03-18 Room:106 Time:May 26 09:45-10:00

Post-perovskite phase boundary of Fe- and Al-bearing MgSiO3

WANG, Xianlong[1*] ; TSUCHIYA, Taku[1]

[1]GRC, Ehime University; ELSI, Tokyo Institute of Technology

The post-perovskite (PPv) phase transition of $MgSiO_3$ bridgmanite (Br) [1,2,3] occurs in the pressure (P) and temperature (T) conditions corresponding to the Earth's D? layer. Therefore, $MgSiO_3$ PPv is believed to be a key mineral to understanding the seismological properties in this layer. However, to date, it is still a challenging subject to determine the phase transition boundary preciously in the geophysically relevant Fe and Al-bearing compositions. Based on the first-principles methods combined with the internally consistent LSDA+U method and the lattice dynamics approach, the high-P and high-T thermodynamics of the $MgSiO_3$ phases are directly calculated with incorporation of 6.25 mol% of Fe^{2+}, $Fe^{3+}Fe^{3+}$, $Fe^{3+}Al^{3+}$, and $Al^{3+}Al^{3+}$ [4,5]. Using calculated free energies, we determine the PPv phase boundaries for Fe and Al-bearing compositions. Our results show that at 2500 K, the $Fe^{3+}Al^{3+}$ and $Fe^{3+}Fe^{3+}$ incorporations span coexisting domains between Br and PPv significantly with lowering the transition pressure, in contrast to the Fe^{2+}- and $Al^{3+}Al^{3+}$-bearing cases.

References:
[1] M. Murakami, K. Hirose, K. Kawamura, N. Sata, and Y. Ohishi, Science **304**, 855 (2004).
[2] A. Oganov, and S. Ono, Nature **430**, 445 (2004).
[3] T. Tsuchiya, J. Tsuchiya, K. Umemoto, and R. M. Wentzcovitch, Earth. Planet. Sci. Lett. **224**, 241 (2004).
[4] J. Tsuchiya, and T. Tsuchiya, Proc. Natl. Acad. Sci. USA **105**, 19160 (2008).
[5] A. Metsue, and T. Tsuchiya, Geophys. J. Int. **190**, 310 (2012).

Keywords: First-principles method, internally consistent LSDA+U, post-perovskite, phase transition

Japan Geoscience Union Meeting 2015
(May 24th - 28th at Makuhari, Chiba, Japan)

SIT03-19 Room:106 Time:May 26 10:00-10:15

New constraints on S-wave velocity structure near the western edge of the Pacific LLSVP

TANAKA, Satoru[1*] ; KAWAKATSU, Hitoshi[2]

[1]JAMSTEC, [2]ERI, Univ. Tokyo

S-wave velocity structure near the edge of the Pacific Large-Low Shear Velocity Province (LLSVP) has been examined by many researchers (e.g., He et al., 2006; He and Wen, 2009; Takeuchi et al., 2008; Idehara et al., 2013). They have mainly used the differential travel times of ScS-S observed by global or local broadband networks (e.g., IRIS GSN, F-net, CNDSN and so on). Here we add the new data of ScS-S and S-SKS travel time data obtained by NECESSArray and a temporal broadband ocean bottom seismograph network in the Philippine Sea by the Stagnant Slab Project (SSP-BBOBS) (Shiobara et al., 2005).

ScS-S anomalies observed by NECESSArray in conjunction with those by F-net, which covers the region beneath the eastern Micronesia, are roughly explained by the existing 3D S-wave models. However, S-SKS anomalies, which are affected by S-waves propagated near the base of the mantle beneath the western Micronesia and the north of New Britain Island, suddenly changes from positive in the eastern area to almost zero or slightly negative in the western, whereas all the models predict large positive anomalies without significant changes. To confirm this S-SKS observation, we further examined ScS-S anomalies observed by the SSP-BBOBS. Some data indicate nearly zero in the corresponding area although the data are scattered and still sparsely distributed. Since a low velocity anomaly beneath the New Guinea Island are confirmed by Takeuchi et al. (2008) and Idehara et al. (2013), our observation suggests that the Pacific LLSVP is separated beneath the north of New Britain Islands. The models of 3D mantle structure are possibly insufficient near the western edge of the Pacific LLSVP.

Acknowledgements. The authors are grateful to the participants of NECESSArray and SP-BBOBS projects and the staffs of IRIS and F-net for providing valuable data.

Keywords: LLSVP, Pacific, S-wave velocity structure, lower mantle

Japan Geoscience Union Meeting 2015
(May 24th - 28th at Makuhari, Chiba, Japan)

SIT03-20 Room:106 Time:May 26 10:15-10:30

On the origin of a stably stratified layer below the CMB inferred from dynamo models

TAKAHASHI, Futoshi[1*]

[1]Department of Earth and Planetary Sciences, Kyushu University

The geodynamo is powered by the two agents, thermal and compositional buoyancy. The former is fueled by secular cooling of the Earth and/or latent heat upon solidification of the inner core, while the latter is by release of the light elements at the inner core boundary with inner core growth. Since these two buoyancy sources should behave differently due to the vast difference of their diffusivity based on the molecular values, double diffusive convection would occur in the Earth's core.

Apart from double diffusive convection, it is inferred from seismic observations that there is a thin stably stratified layer of O(100) km below the core-mantle boundary. However, it is not well constrained whether the origin of stable stratification is thermal or compositional. Here we investigate effects of a stable layer on dynamo action driven by double diffusive convection. Stably stratified layer is imposed by giving a sub-adiabatic temperature gradient. Thickness of the stable layer is assumed to be 10 % of the core radius. It is found that strength of the dynamo-generated magnetic field is significantly reduced by the thin stable layer in case of dipolar dynamos. On the other hand, the magnetic field is strengthened with the stable layer in case of weak multi-polar dynamos, consistent with a previous study. We discuss mechanisms responsible for such a difference and implications for the origin of the stably stratified layer.

Keywords: dynamo, core, stable stratification, double diffusive convection

Japan Geoscience Union Meeting 2015
(May 24th - 28th at Makuhari, Chiba, Japan)

SIT03-21 Room:106 Time:May 26 10:30-10:45

Magnetic Rossby waves in the Earth's core

HORI, Kumiko[1*] ; JONES, Chris[1] ; TEED, Rob[3]

[1]Department of Applied Mathematics, University of Leeds, UK, [2]STEL, Nagoya University, [3]DAMTP, University of Cambridge, UK

Magnetohydrodynamic waves in rapidly rotating planetary cores can produce several secular variations of the planetary magnetic field. Some axisymmetric modes, including the torsional Alfven waves, are thought to be responsible for certain observed features of the Earth's core dynamics and the geomagnetic variation. It is, on the other hand, possible for other waves to lead to the nonaxisymmetric variations. A potential candidate is the magnetic Rossby wave, which migrates in the azimuthal direction along the internal toroidal field. This can be related to the westward drift of the geomagnetic field, which has been observed in the Atlantic hemisphere for the past hundred years. Though the drift has commonly been believed to reflect advection due to large-scale lateral flows beneath the top of the core, propagation of the waves excited within the core may also account for it. This was originally proposed by Hide (1966), who showed that a slow mode of magnetic Rossby waves, sometimes called a slow MC-Rossby mode, could propagate westward on timescales of hundreds years.

To investigate whether this mode can be relevant in the Earth's core, we extend Hide's linear theory to quasi-geostrophic cylinders and explore nonlinear dynamo simulations in rotating spherical shells. By performing tempo-spatial spectral analyses, we identify slow MC-Rossby waves that propagate at the correct speed, given by the Alfven and Rossby speeds, with respect to the mean zonal flow. The result indicates that this mode could be excited in the planetary fluid core and that the wave propagation may indeed play a role in the magnetic drift. Taking geomagnetic drift speeds, the theory suggests the internal toroidal field of about 10 mT at the mid core radius. This could give a framework for inferring the physical properties in the fluid core, in terms of nonaxisymmetric waves.

Japan Geoscience Union Meeting 2015
(May 24th - 28th at Makuhari, Chiba, Japan)

SIT03-22 Room:106 Time:May 26 11:00-11:15

Liquid iron alloys with light elements at outer core conditions by first-principles calculation

UMEMOTO, Koichiro[1*] ; HIROSE, Kei[2]

[1]Earth-Life Science Institute, Tokyo Institute of Technology, [2]ELSI, TITECH; OELE, JAMSTEC

Since the density of the outer core deduced from seismic data is about 10% lower than that of pure iron at core pressures and temperatures (P-T), it is widely believed that the outer core includes one or more light elements. Although intensive experimental and theoretical studies have been performed so far, the light element in the core has not yet been identified. Comparison of the density and sound velocity of liquid iron alloys with observations, such as the PREM, is a promising way to determine the species and quantity of light alloying component(s) in the outer core. Here we report the results of a first-principles molecular dynamics study on liquid iron alloyed with different concentrations of light elements, in order to clarify the effects of their impurities on the liquid density and sound velocity under outer core P-T conditions. We also discuss validity of empirical Birch's law between density and sound velocity in liquid iron alloys.

Keywords: outer core, liquid iron alloys, first principles

Japan Geoscience Union Meeting 2015
(May 24th - 28th at Makuhari, Chiba, Japan)

SIT03-23 Room:106 Time:May 26 11:15-11:30

Sound velocity measurements of liquid Fe-C alloy under high pressure

NAKAJIMA, Yoichi[1*] ; IMADA, Saori[2] ; HIROSE, Kei[2] ; KOMABAYASHI, Tetsuya[3] ; OZAWA, Haruka[4] ; TATENO, Shigehiko[2] ; KUWAYAMA, Yasuhiro[5] ; TSUTSUI, Satoshi[6] ; BARON, Alfred[1]

[1]RIKEN, SPring-8 Center, [2]Earth-life science institute, Tokyo Institute of Technology, [3]School of GeoSciences, The University of Edinburgh, [4]Japan Agency for Marine-Earth Science and Technology, [5]Geodynamics Research Center (GRC), Ehime University, [6]Japan Synchrotron Radiation Research Institute

The liquid Earth's outer core consists predominantly of iron with c.a. 10 wt.% lighter elements, such as hydrogen, carbon, oxygen, silicon, and sulfur. Other terrestrial planets such as Mars, Mercury and Venus are also similar to the Earth in that they have central metallic cores, which are considered to be at least partially molten. Popular models for those planetary cores also favor the presence of lighter elements. The nature of the light elements is important for understanding the core formation processes and the present core structure and dynamics in terrestrial planets, both of which are still not well understood. The seismic wave speed is the primary information on the Earth's core. The sound velocity of liquid Fe alloying with light-elements is therefore key to constrain the lighter component in the Earth's core and provide a reference for future surveys of other planets. Recently we have developed the techniques for inelastic X-ray scattering (IXS) measurements combined with diamond-anvil cell (DAC) experiments at the SPring-8 IXS spectrometers in order to investigate sound velocities of liquid Fe alloying with light-elements under the high pressure and high temperature conditions relevant to planetary cores. We determined the sound velocity of liquid Fe-C alloy up to 70 GPa. We will discuss the effect of carbon on the sound velocity of liquid iron and implications for planetary cores.

Keywords: sound velocity, light element in the core, liquid iron carbide, high pressure

Japan Geoscience Union Meeting 2015
(May 24th - 28th at Makuhari, Chiba, Japan)

SIT03-24 Room:106 Time:May 26 11:30-11:45

Melting experiments in the system Fe-FeS at core pressures

MORI, Yuko[1*] ; TATENO, Shigehiko[2] ; HIROSE, Kei[2] ; MORARD, Guillaume[3] ; OHISHI, Yasuo[4]

[1]Dept. of Earth & Planetary Sciences, Tokyo Institute of Technology, [2]Earth-Life Science Institute, Tokyo Institute of Technology, [3]IMPMC, Universite Pierre-et-Marie-Curie, [4]Japan Synchrotron Radiation Research InstituteJ

Most of the Earth's core is iron and nickel alloy. However, the density of the core acquired from Preliminary reference Earth model (PREM) is smaller than that of pure iron. The amount of deficit is 6-10 wt % at the outer core and 1-3 wt % at the inner core. To explain this deficit, the core might contain one or more light elements (H, C, N, O, Si, S).

S is depleted in the crust and mantle compared to other volatile elements (Poirier ,1994). Moreover, iron meteorites contain S (Chabot, 2004), thus we focus on S. In order to discuss the composition of the core, the phase diagram is important. The bulk core composition must be Fe-rich side at inner core boundary (ICB) because the outer core incorporates larger amounts of light element than the inner core. Fe-FeS phase diagram is determined by X-ray diffraction (XRD) pattern (e.g. Morard et al. 2008) or chemical analysis of recovered sample (e.g. Kamada et al. 2012). However, no accurate determination of the eutectic composition has been obtained by XRD. On the other hand, constraining by chemical analysis has not been done using sample recovered from core pressure. Thus, we examine Fe-S phase diagram at higher pressure.

High pressure and temperature (P-T) conditions were generated in a laser-heated diamond-anvil cell. We used Fe-7.5, 13.5 wt.% S foil as a starting material. Angle-dispersive in situ X-ray diffraction (XRD) measurements at high P-T were conducted at BL10XU, SPring-8. The textural and chemical characterizations of recovered samples were made with a field-emission-type scanning electron-microprobe (FE-SEM) equipped with energy dispersive x-ray spectrometry (EDS) and with a field-emission-type electron probe microanalyzer (FE-EPMA). Cross sections of samples were carefully examined by combining a focused Ga ion beam (FIB) with FE-SEM.

From quantitative analysis, we observed the trend that the amount of S in melt decreases and that the amount of S in the solid Fe increases with increasing pressure.

Obseving the sample using Fe-7.5 wt % S by SEM, we can see the 3 textures; melt, solid Fe, subsolidus phase. Melt includes more S than solid Fe. The content of S in liquid is between 12.5 and 10.4 wt. % in the range of 38-138 GPa. The eutectic composition is expected to have S than molten iron. Moreover, according to the experiment using S rich starting material, the texture of recovered sample contain melt ,Fe3S, subsolidus phase. The S content in melt is larger than that in eutectic composition.Using both of S-rich and S-poor starting material, we can constrain the eutectic composition.

Assuming that the negative pressure dependence of S content in melt is retained up to ICB pressure, the content of S in liquid Fe at ICB pressure is lower than 10 wt %. The S amount required to explain core density deficit (CDD) is 11.9-13.9 wt.% at outer core and 6-6.6 wt. % at inner core (Sata et al. 2010) . In this condition, the S content of eutectic composition is more than 11.9 wt.%. However, this value is great comparing to the eutectic composition expected from this study. Therefore, S is not the only light element inthe Earth's core.

Keywords: High pressure and temperature, melting experiments, the Earth's core, light element, core density deficit

Japan Geoscience Union Meeting 2015
(May 24th - 28th at Makuhari, Chiba, Japan)

SIT03-25 Room:106 Time:May 26 11:45-12:00

Inner core dynamics inferred from grain growth of epsilon-iron

YAMAZAKI, Daisuke[1*] ; TSUJINO, Noriyoshi[1] ; YONEDA, Akira[1] ; YOSHINO, Takashi[1] ; HIGO, Yuji[2]

[1]Okayama Univ., [2]JASRI

The inner core is thought to be composed of Fe-Ni alloy with hcp structure based on the high pressure experiments (Tateno et al., 2012) and hence the physical properties of hcp iron (epsilon-iron) are keys for understanding the dynamics of the inner core. Recent seismic observations suggest the variation in grain size in the inner core (Monnereau et al., 2010). It is important to understand the variation in grain size for constraints of the dynamics of the inner core because grain size is controlled by the growth rate and growth rate gives us information on time scale of the inner core growth and/or deformation. In this study, we experimentally determine the grain growth rate of epsilon-iron to understand the dynamics of inner core.

epsilon-iron is only stable at high pressure and it is unquenchable to an ambient condition. Therefore, in this study, we conduct in situ high pressure experiments to determine the grain growth rate of epsilon-iron. We prepared polycrystalline iron of starting material by multi-directional forging (MDF) on highly purity iron rod to avoid oxidation during sintering. In the high pressure experiment, the starting materials was compressed in a Kawai-type high pressure apparatus equipped with sintered diamond anvils with 1.0 truncated edge length at BL04B1, SPring-8. At the pressure of 50-60 GPa, sample was heated for several hours to determine the grain growth rates. Grain growth can be detected by the reduction of number of diffraction spots on the two-dimensional detector with monochromatic X-ray (Offerman et al., 2002) with annealing time.

In the experiments, we observed the reduction of the number of diffracted spots, meaning that grain growth occurs during annealing experiments. For example, the number of diffraction spots reduced to 50 % after annealing at 1300 K for two hours. By extrapolating the present data, we may constrain the translation dynamics of the inner core (Alboussiere et al., 2010) in comparison with seismic observation.

Monnereau, M., Calvet, M., Margerin, L., Souriau, A. (2010) Lopsided growth of earth's inner core, Science, 328, 1014-1017.

Alboussiere, T., Deguen, R., Melzani, M. (2010) Melting-induced stratification above the earth's inner core due to convective translation, Nature, 466, 744-747.

Offerman, S. E., van Dijk, N. H., Sietsma, J., Grigull, S., Lauridsen, E. M., Margulies, L., Poulsen, H. F., Rekveldt, M., van der Zwaag, S. (2002) Grain nucleation and growth during phase transformations, Science, 298, 1003-1005.

Tateno, S., Hirose, K., Komabayashi, T., Ozawa, H., Ohishi, Y. (2012) The structure of Fe-Ni alloy in earth's inner core, Geophy. Res. Lett., 39, L12305.

Japan Geoscience Union Meeting 2015
(May 24th - 28th at Makuhari, Chiba, Japan)

SIT03-P01 Room:Convention Hall Time:May 26 18:15-19:30

Continuous measurements of electrical conductivity of synthetic peridotite under changing temperature: Melting effect

SUEYOSHI, Kenta[1*] ; HIRAGA, Takehiko[1]

[1]Earthquake Research Institute, The University of Tokyo

Transport properties of the mantle (ex. electrical conductivity, viscosity, and seismic attenuation) sharply changes during ascend of the mantle especially at around mantle solidus. Electrical conductivity is considered to be the most sensitive property to the presence of partial melt. To understand how partial melting changes the conductivity of ascending mantle (ex. mid-ocean ridge), we measured the electrical conductivity of synthesized peridotite samples, which have different manners of melting with temperature, during slow increases and decreases in temperature under atmospheric pressure.

Three types of samples, forsterite (80%) + diopside (20%), forsterite (95%) + diopside (5%) and forsterite (50%) + enstatite (40%) + diopside (10%) with addition of 0.5% spinel, were synthesized from $Mg(OH)_2$, SiO_2, $CaCO_3$ and $MgAl_2O_4$ powders with particle size of $<$50 nm. We continuously measured the electrical conductivity of these samples at temperature range from 1100 ℃ to 1400 ℃. Microstructures of the samples quenched from above solidus were observed by scanning electron microscopy (SEM) in order to measure the melt fraction.

The electrical conductivity at well below ($>$50 ℃) solidus of the forsterite + diopside samples exhibited a linear distribution in their Arrhenius plots indicating that a single mechanism controls. Such linear relationship was no longer observed at higher temperature regime exhibiting its exponential increase until the temperature reached to produce a phase assembly of forsterite + melt. In addition, the grain size dependence on electrical conductivity disappeared at temperature between 1350 ℃ and 1360 ℃, indicating that the effective conductive path changed from grain boundary to other path. The result indicates that there is a phase assembly of forsterite + diopside + melt phase at around 1360 ℃ which has not been appeared in the previously reported phase diagram (Kushiro and Schairer, 1963).

Monotonic increase of electrical conductivity was observed above solidus of the forsterite + enstatite + diopside + spinel sample, and such increment is considered to be strongly related melt fraction changing with temperature, which is supported from SEM observation.

Keywords: electrical conductivity, peridotite, partial melting, melt fraction

Japan Geoscience Union Meeting 2015
(May 24th - 28th at Makuhari, Chiba, Japan)

SIT03-P02 Room:Convention Hall Time:May 26 18:15-19:30

Measurement of single crystal elasticity of Gold (Au) under high temperature and high pressure

YONEDA, Akira[1*] ; FUKUI, Hiroshi[2] ; HIRAO, Naohisa[3] ; KAMADA, Seiji[4] ; BARON, Alfred[5]

[1]ISEI, Okayama Univ., [2]Univ. of Hyougo, [3]JASRI, [4]Graduate school of Science, Tohoku University, [5]RIKEN

Single crystal elasticity of gold (Au) has been measure by inelastic X ray scattering method under high pressure. A few tens micrometer Au single crystal was prepared from a large commercial crystal by using FIB technique. The small crystal was placed inside a gasket hole of DAC apparatus. We succeeded to measure single crystal elasticity at 0.8 GPa and 3.2 GPa; the pressures were determined by the Ruby scale. ˜100 peaks were observed at each pressure, and used to constrain the three independent constants of C_{11}, C_{12}, and C_{44}. The resulted elastic constants are consistent with the previous data at ambient pressure.

We observed that C_{11} and C_{44} increase with increasing pressure, and C_{12} decreases with increasing pressure. We will expand the pressure range and temperature range of the measurement to establish the equation of state of gold with unprecedented accuracy.

Keywords: Gold, single crystal, elasticity, high pressure

Japan Geoscience Union Meeting 2015
(May 24th - 28th at Makuhari, Chiba, Japan)

SIT03-P03 Room:Convention Hall Time:May 26 18:15-19:30

High temperature generation using semiconductor diamond heater at high pressure

ITO, Eiji[1*] ; YONEDA, Akira[1] ; XIE, Longjian[1] ; TSUJINO, Noriyoshi[1]

[1]Institute for Study of the Earth's Interior, Okayama University

Melting relations of the Earth materials are information essentially important to clarify the early differentiation and evolution of the Earth. Nevertheless melting experiments using the Kawai-type apparatus under mid mantle conditions are impossible because of limited temperature generation. Following Shatsky et al. (2009), we have tried to generate temperatures higher than 3500 K adopting B-doped semiconductor diamond heater. In order to carry out melting experiments at higher than 50 GPa, we adopt sintered diamond anvils. Temperature (T) is estimated by extrapolating a T-W (power) curve constructed up to 2600 C based on the W/re thermocouple measurement. Our T-generation reached ca. 4700 C at 55GPa.

Keywords: High temperature generation, Semiconductor diamond heater, Kawai-type apparatus, sintered diamond

Japan Geoscience Union Meeting 2015
(May 24th - 28th at Makuhari, Chiba, Japan)

SIT03-P04 Room:Convention Hall Time:May 26 18:15-19:30

Numerical Simulation on Subduction of the Pacific Plate into Northeast China and the Seismogenic Mechanism of Earthquake

JIAO, Mingruo[1*] ; BO, Zhang[1]

[1]Earthquake Adimistration of Liaoning Province, Shenyang, 110034, P.R.China

The Pacific Plate is subducted into Northeast China up to 660km deep, leading to a series of deep earthquakes in Hunchun zones of Jilin province, which was noticed by seismologists in the past. As the only deep-earthquake belt in China, its occurrence-time, locations and magnitudes are closely associated with Japan trench earthquakes and shallow earthquakes in Northeast China. Until now, seismologists attached great importance to this phenomenon and researched it in various aspects. On the one hand, research results confirmed the above phenomenon. On the other hand, masses of important results were obtained including the structure of the Pacific subducting plate, lithosphere structure in Northeast China, the earthquake focal mechanism and the seismic dynamic mechanism about the deep and shallow earthquakes. But until now, there is seldom systematic research about the relationship among the Pacific plate, deep and shallow earthquakes using numerical simulation method. Therefore, this paper will study their relationships and furtherly explore the tectonic stress field and dynamics environment in Northeast China.

Based on the geology data and the seismic velocity structure in Northeast China, we built the 2D vertical model along the 45 degree latitude ranging from 104 to 144 degree longitude with 0-660km deep to simulate the Pacific plate subducting to Northeast China using finite element numerical simulation method. According to motion rate of the Pacific plate to the Eurasian plate, the boundary conditions are given. The model with the typical tectonic belts, such as Tanlu fault, can explain the earthquake mechanism and study the stress fields and displacement fields. Besides the relationship between fault belts and shallow earthquakes is discussed.Through numerical simulation and comprehensive analysis, some conclusions are obtained as follows:

(1) The Pacific plate subduction into Northeastern China is the main dynamic resource causing a series of deep-focal and shallow-focal earthquakes. The stress field shows that there are two main areas of stress concentration under the subduction of the Pacific plate. It can help us to explain the relationship about the seismogenic mechanism between deep and shallow earthquakes.

(2) The displacement field and deformation field are given. The results show the displacement field and deformation field are controlled by the Pacific plate subduction rates. Exist of low velocity medium in the middle crust layer is in favor of the occurrence of the shallow earthquakes.

Keywords: numerical simulation, subduction of the Pacific plate, deep and shallow earthquakes, Northeast China

Japan Geoscience Union Meeting 2015
(May 24th - 28th at Makuhari, Chiba, Japan)

SIT03-P05 Room:Convention Hall Time:May 26 18:15-19:30

S-velocity structure of the crust and uppermost mantle of East Asia from ambient seismic noise

WITEK, Michael[1*] ; NING, Shuoxian[1] ; KANG, Tae-seob[2] ; VAN DER LEE, Suzan[1] ; CHANG, Sung-joon[3] ; NING, Jieyuan[4]

[1]Northwestern University, [2]Pukyong National University, [3]Kangwon National University, [4]Peking University

We have collected continuous vertical-component broadband data from 1109 seismic stations in regional networks across China, Korea, and Japan for the year 2011, and we have measured over half a million Rayleigh wave group velocity dispersion curves from one-year stacks of station-pair ambient seismic noise cross-correlations. The Rayleigh wave group velocity dispersion curves are regionalized on a tessellated spherical shell grid in the period range 10 to 50 s to produce maps of Rayleigh wave group velocity distributions. Maps at 10 seconds period match well with geologic features at the surface. In particular, we observe low group velocities in the Songliao, Bohai Bay, Sichuan, Ordos, Tarim, and Junggar Basins in China, and the Ulleung and Yamato Basins in the East Sea (Sea of Japan). Higher group velocities are observed in regions with less sediment cover. At periods around 30 s, we observe group velocity decreases going from east to west in China, representing an overall trend of crustal thickening due to the collision between the Indian and Eurasian plates. The Ordos and Sichuan blocks show higher group velocities relative to the eastern margin of the Tibetan Plateau, possibly reflecting low temperatures in these cratons. Using the Rayleigh wave group velocity distributions, we have performed 1D linear inversions at each node on the spherical shell grid to retrieve S-velocity perturbations with respect to the reference model LITHO1.0 of Pasyanos *et al.* (2014). This has allowed us to construct a 3D model of the crust and uppermost mantle for East Asia. We observe large-scale lateral variation in the crust compared to the LITHO1.0 model. From 50 to 100 km depth, we observe a low-velocity mantle wedge underneath Japan and the Strait of Korea, and at 100 km depth we see a general trend of increasing S-velocities from east to west, possibly reflecting temperature/water content variations in the mantle.

Keywords: East Asia, tomography, ambient noise

Japan Geoscience Union Meeting 2015
(May 24th - 28th at Makuhari, Chiba, Japan)

SIT03-P06 Room:Convention Hall Time:May 26 18:15-19:30

One-dimensional shear velocity structure beneath Okinawa trough inferred from surface wave phase velocity

KOBAYASHI, Reiji[1*] ; FUKUDA, Keisuke[2] ; TASAKI, Naoko[3] ; ETOH, Ayano[4]

[1]Kagoshima University, [2]Kagoshima University, [3]Kagoshima University .Now at JMSDF, [4]Kagoshima University. Now at Kasaki Clinic

Structures beneath back-arc basins or marginal seas are as important as those just beneath island arcs to understand the whole systems of subduction zones. However number of studies on structure beneath back-arc basins is limited because of few seismic stations in back arc basin.

This study focuses on the structures beneath Okinawa trough. Philippine sea plate is subducting along the Ryukyu trench and the Ryukyu arc is an island arc of this subduction zone. Okinawa trough is located in backarc region of Ryukyu arc and is considered to be a region of backarc spreading. Crustal structure along the Okinawa trough has been investigated by the Japan Coast Guard (e.g. Horiuchi et al., 2011) and the Moho depth has been obtained. For the upper mantle structure, Nakamura et al. (2003) inferred three dimensional P and S-wave structure by body wave tomography and several studies inferred three dimensional S-wave tomography as a surrounding part of continent by surface wave tomography (e.g., Huang and Zhao, 2006). However, the mantle dynamics beneath the Okinawa trough has not been well imaged.

As the first step of investigation of the mantle dynamics beneath the Ryukyu arc and Okinawa trough, we inferred one-dimensional shear-wave velocity structure of crust and uppermost mantle beneath the Okinawa trough. We also inferred that beneath East China Sea continental shelf.

We measured phase velocities of Rayleigh and Love waves by two-station method and obtained dispersion curves. We used stations of F-net of National Research Institute for Earth Science and Disaster Prevention (NIED), China Digital Seismograph Network (CDSN), and Global Seismograph Network (GSN).

We then inferred one-dimensional shear-wave average structure along the path by genetic algorithm. We assumed radial anisotropy in uppermost mantle (Moho to 220 km) and isotropy in other layers.

Shear wave velocities just below the Moho beneath the Okinawa trough is significantly lower than that beneath the continental shelf. It may suggest partial melting due to upwelling beneath the Okinawa trough. However, the velocities around 220 km is higher than that beneath the continental shelf, suggesting that origin of the upwelling is not deep. The upwelling could be a passive flow like that beneath mid-ocean ridge. SV velocities beneath western part of the Okinawa trough is lower than SH velocities, while SV and SH velocities beneath eastern part are similar to each other. This radial anisotropy may be caused by the shape of the cracks of partial melt or preferred orientations of mantle minerals.

Keywords: Okinawa trough, backarc spreading, seismic structure, surface wave

Japan Geoscience Union Meeting 2015
(May 24th - 28th at Makuhari, Chiba, Japan)

SIT03-P07 Room:Convention Hall Time:May 26 18:15-19:30

P-wave velocity anomalies of the plume beneath the French Polynesia

OBAYASHI, Masayuki[1*] ; YOSHIMITSU, Junko[1] ; SUGIOKA, Hiroko[1] ; ITO, Aki[1] ; ISSE, Takehi[2] ; SHIOBARA, Hajime[2] ; SUETSUGU, Daisuke[1]

[1]D-EARTH, JAMSTEC, [2]ERI, Univ. Tokyo

The French Polynesian region is characterized by positive topographic anomalies of 700 m, a concentration of hotspot chains. Many seismic tomography results show a broad low-velocity anomaly in the lower mantle continued from the base of the mantle. These observations suggest that a large-scale mantle flow rises from the bottom of the mantle beneath the region. Joint Japanese-French broadband seismological observations were performed from 2001 to 2005 with 10 island stations from the Polynesian PLUME project (Barruol et al. 2002) and 10 broadband ocean bottom seismometers (BBOBSs) from the Polynesian BBOBS project (Suetsugu et al. 2005). A P-wave

tomography using the data from these projects revealed that large-scale low-velocity anomalies (on the order of 1000 km in diameter) from the bottom of the mantle become smaller-scale low-velocity anomalies (on the order of 100 km in diameter) at the depth of about 1000 km. However the connection of the small-scale low-velocity anomalies to the surface hotspots was not unrevealed because of the poor resolution in the upper mantle.

A new P-wave tomography with better resolution in the upper mantle was obtained by adding data from BBOSBSs around Society Islands deployed along the TIARES project during 2009 - 2010 (Suetsugu et al. 2012) and by taking the finite frequency effect into account for the frequency-depended differential travel times. The frequencydepended differential travel times were measured by multi-band cross correlating P waveforms. The new P-wave tomography shows strong low-velocity anomalies beneath the Society Islands and Pitcairn in the upper mantle although they do not extend to the 660-km discontinuity. This model also shows that small-scale low-velocity anomalies in the uppermost lower mantle. The low-velocity anomalies in the depth range about 550 - 900 km are smaller both in lateral area and amplitude than those in most of the upper mantle and the lower mantle. The velocity patterns are well correlated each other in the depth range but are not correlated with the patterns above and below, indicating the mantle beneath the French polynesia can be divided into 3 layers in terns of radial correlation.

Keywords: Tomography, Plume, Mantle, French Polynesia